Chapter 6

Solution of the Transonic Small Disturbance Equation

6.1 Introduction

Murman and Cole provided the algorithm for solving the Transonic Small Disturbance equation. This was one of the most significant events in the history of computational fluid dynamics. Their algorithm used type dependent differencing, depending upon the whether the flow was locally sub or supersonic. This procedure became the key element used for the development of algorithms for solving the Full Potential and Euler equations.

6.2 The Murman-Cole Method

The Transonic Small Disturbance equation governing irrotational and isentropic flow near Mach one past slender bodies can be written in two dimensions as

$$\left[1-M_\infty^2-(\gamma+1)M_\infty^2\frac{\phi_x}{V_\infty}\right]\phi_{xx}+\phi_{yy}=0$$

or $$A(\hat{\phi}_x)\phi_{xx}+\phi_{yy}=0,\quad with\quad A(\hat{\phi}_x)=1-M_\infty^2-(\gamma+1)M_\infty^2\frac{\phi_x}{V_\infty}$$

where M_∞ is the free stream Mach number and ϕ represents the small disturbance velocity potential, $u'=\frac{\partial\hat{\phi}}{\partial x}=\phi_x$, $v=v'=\frac{\partial\hat{\phi}}{\partial y}=\phi_y$, $u=V_\infty+u'$ and V_∞ is the free stream velocity. The equation is non-linear because the coefficient A before the $\hat{\phi}_{xx}$ term is a function of $\hat{\phi}$ itself. The equation can be elliptic if $A>0$ or hyperbolic if $A<0$. At sonic points within the flow $A=0$ and A changes sign across shock wave discontinuities. The speed of sound at sonic points, for which the flow speed equals the local speed of sound, is given by $a^*=V_\infty\left(1+\frac{1-M_\infty^2}{(\gamma-1)M_\infty^2}\right)$. Using the "jump" relation procedure presented in Chapter 2 for discontinuities across surface $f(x)=x-x_0$, it can be shown (see Section 2.4.3.4) that $\frac{u_1+u_2}{2}=a^*$, where u_1 and u_2 are the x – components of velocity on either side of the shock wave.

There was an exceptionally large effort to solve the Transonic Small Disturbance equation as aircraft engines became powerful for transonic flight following World War II.

These numerical efforts applied central differencing that was successful for solving the model elliptic equation in the Chapter 5, but proved disastrous when the flow became supersonic and the governing Transonic Small Disturbance equation became hyperbolic. Murman and Cole, working together at Boeing in Seattle one summer (1971), found the solution key to this equation. They changed the differencing of the $\hat{\phi}_{xx}$ term from central to backward whenever the flow became supersonic. They used the local value of A to determine when to make the switch. A couple of years later they also presented rules for differencing the equations at sonic and shock points. Their breakthrough procedure was like a shot heard round the world. Industry, universities and government laboratories in aeronautical research quickly adopted their numerical procedure. It is given below in four parts.

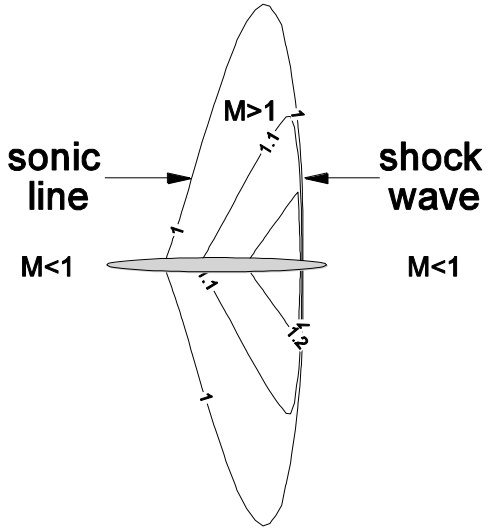

Figure 6.1 Transonic flow past a thin airfoil

(i) Subsonic flow region - $A_{i,j} > 0$ - use centered difference approximations for both terms.

$$A_{i,j}\frac{D_{xx}\cdot}{\Delta x^2}\hat{\phi}_{i,j} + \frac{D_{yy}\cdot}{\Delta y^2}\hat{\phi}_{i,j} = 0$$

where

$$\frac{D_{xx}\cdot}{\Delta x^2}\phi_{i,j} = \frac{\phi_{i+1,j} - 2\phi_{i,j} + \phi_{i-1,j}}{\Delta x^2}$$

$$\frac{D_{yy}\cdot}{\Delta y^2}\phi_{i,j} = \frac{\phi_{i,j+1} - 2\phi_{i,j} + \phi_{i,j-1}}{\Delta y^2}$$

and

$$A_{i,j} = 1 - M_\infty^2 - (\gamma+1)\frac{M_\infty^2}{V_\infty}\frac{\phi_{i+1} - \phi_{i-1}}{2\Delta x}$$

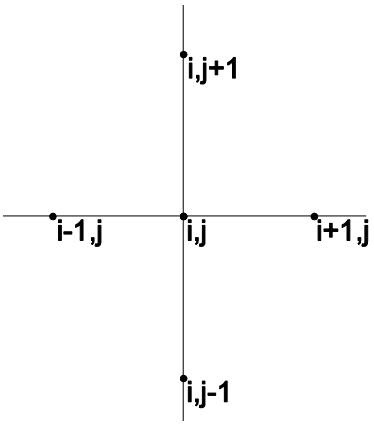

Figure 6.2 Subsonic mesh stencil

(ii) Supersonic flow region - $A_{i,j} < 0$ - use a backward difference approximation for the $\hat{\phi}_{xx}$ term.

$$A_{i-1,j}\frac{D_{xx}\cdot}{\Delta x^2}\hat{\phi}_{i-1,j} + \frac{D_{yy}\cdot}{\Delta y^2}\hat{\phi}_{i,j} = 0$$

where

$$\frac{D_{xx}\cdot}{\Delta x^2}\hat{\phi}_{i-1,j} = \frac{\hat{\phi}_{i,j} - 2\hat{\phi}_{i-1,j} + \hat{\phi}_{i-2,j}}{\Delta x^2}$$

$$\frac{D_{yy}\cdot}{\Delta y^2}\hat{\phi}_{i,j} = \frac{\hat{\phi}_{i,j+1} - 2\hat{\phi}_{i,j} + \hat{\phi}_{i,j-1}}{\Delta y^2}$$

and

$$A_{i-1,j} = 1 - M_\infty^2 - (\gamma+1)\frac{M_\infty^2}{V_\infty}\frac{\phi_i - \phi_{i-2}}{2\Delta x}$$

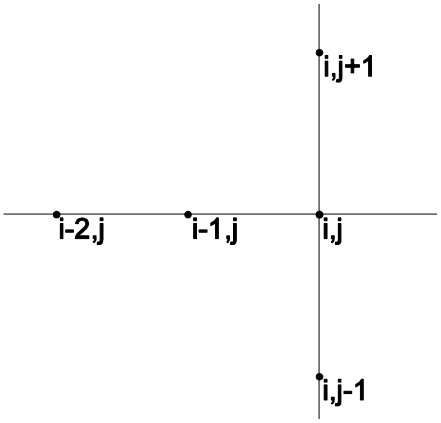

Figure 6.3 Supersonic stencil

(iii) Sonic points - $A_{i-1,j} > 0$ and $A_{i,j} < 0$ - omit the $\hat{\phi}_{xx}$ term.

$$\frac{D_{yy}\cdot}{\Delta y^2}\hat{\phi}_{i,j} = 0$$

(iv) Shock points - $A_{i-1,j} < 0$ and $A_{i,j} > 0$ -include the $\hat{\phi}_{xx}$ term twice.

$$A_{i,j}\frac{D_{xx}\cdot}{\Delta x^2}\hat{\phi}_{i,j} + A_{i-1,j}\frac{D_{xx}\cdot}{\Delta x^2}\hat{\phi}_{i-1,j} + \frac{D_{yy}\cdot}{\Delta y^2}\hat{\phi}_{i,j} = 0$$

The above four different type dependent difference approximations can be combined into a single difference equation using the following switch

$$\mu_{i,j} = \begin{cases} 0 & if\ A_{i,j} > 0 \\ 1 & if\ A_{i,j} < 0 \end{cases}$$

The Murman-Cole method then becomes

$$(1-\mu_{i,j})A_{i,j}\frac{D_{xx}\cdot}{\Delta x^2}\hat{\phi}_{i,j} + \mu_{i-1,j}A_{i-1,j}\frac{D_{xx}\cdot}{\Delta x^2}\hat{\phi}_{i-1,j} + \frac{D_{yy}\cdot}{\Delta y^2}\hat{\phi}_{i,j} = 0$$

The above equation is solved using Gauss-Seidel Line Relaxation (see Section 5.3).

$$(1-\mu_{i,j}^n)A_{i,j}^n\frac{\hat{\phi}_{i+1,j}^n-2\hat{\phi}_{i,j}^{n+1}+\hat{\phi}_{i-1,j}^{n+1}}{\Delta x^2}+\mu_{i-1,j}^n A_{i-1,j}^n\frac{\hat{\phi}_{i,j}^{n+1}-2\hat{\phi}_{i-1,j}^{n+1}+\hat{\phi}_{i-2,j}^{n+1}}{\Delta x^2}+\frac{\hat{\phi}_{i,j+1}^{n+1}-2\hat{\phi}_{i,j}^{n+1}+\hat{\phi}_{i,j-1}^{n+1}}{\Delta y^2}=0$$

A vertical line of points, $\left[\hat{\phi}_{i,J}^{n+1},\hat{\phi}_{i,J-1}^{n+1},\hat{\phi}_{i,J-2}^{n+1},\cdots,\hat{\phi}_{i,2}^{n+1},\hat{\phi}_{i,1}^{n+1}\right]^T$, is solved simultaneously at a time. The line solution is swept through the flow field in the i direction. (Note that at $i=2$ the stencil of mesh points will extend beyond the left boundary, to include a non-existent point at $i=0$. The flow will be subsonic here. Thus at $i=2$ the supersonic term should be dropped from the above equation.) The updated values at $n+1$ replace those at n during the sweep for all i,j. The i^{th} line of the tridiagonal matrix equation being solved is shown below, after moving the terms known from previous line solutions to the right hand side of the equation.

$$(1-\mu_{i,j}^n)A_{i,j}^n\frac{-2\hat{\phi}_{i,j}^{n+1}}{\Delta x^2}+\mu_{i-1,j}^n A_{i-1,j}^n\frac{\hat{\phi}_{i,j}^{n+1}}{\Delta x^2}+\frac{\hat{\phi}_{i,j+1}^{n+1}-2\hat{\phi}_{i,j}^{n+1}+\hat{\phi}_{i,j-1}^{n+1}}{\Delta y^2}=$$
$$-(1-\mu_{i,j}^n)A_{i,j}^n\frac{\hat{\phi}_{i+1,j}^{n}+\hat{\phi}_{i-1,j}^{n+1}}{\Delta x^2}-\mu_{i-1,j}^n A_{i-1,j}^n\frac{-2\hat{\phi}_{i-1,j}^{n+1}+\hat{\phi}_{i-2,j}^{n+1}}{\Delta x^2}$$

The terms can be combined into the following standard tridiagonal form for solution,

$$b_{i,j}\hat{\phi}_{i,j+1}^{n+1}+a_{i,j}\hat{\phi}_{i,j}^{n+1}+c_{i,j}\hat{\phi}_{i,j-1}^{n+1}=f_{i,j}$$

where $f_{i,j}$ represents the right hand side of the equation given above. The resulting tridiagonal matrix equation has the form shown in Sec.5.3.2. The sweep through the mesh, from left to right, is then repeated until the solution converges the absolute value of the residual $\left|R_{i,j}^n\right|$ to an acceptable value, where

$$R_{i,j}^n=(1-\mu_{i,j}^n)A_{i,j}^n\frac{D_{xx}\cdot}{\Delta x^2}\hat{\phi}_{i,j}^n+\mu_{i-1,j}^n A_{i-1,j}^n\frac{D_{xx}\cdot}{\Delta x^2}\hat{\phi}_{i-1,j}^n+\frac{D_{yy}\cdot}{\Delta y^2}\hat{\phi}_{i,j}^n$$

6.3 Stability of the Murman-Cole Method

6.3.1 Subsonic Flow Case Stability

Consider the equation in the linearized form $A\phi_{xx}+\phi_{yy}=0,\ \ with\ \ A>0$, and differenced as follows

$$A\frac{\hat{\phi}_{i+1,j}^n-2\hat{\phi}_{i,j}^{n+1}+\hat{\phi}_{i-1,j}^{n+1}}{\Delta x^2}+\frac{\hat{\phi}_{i,j+1}^{n+1}-2\hat{\phi}_{i,j}^{n+1}+\hat{\phi}_{i,j-1}^{n+1}}{\Delta y^2}=0$$

We take $\phi_{i,j}=ce^{i(k_x x+k_y y)}$ as a test component of the solution and G as the amplification factor for advancing the solution by one iteration step from n to $n+1$ in the relaxation

index direction. Upon substitution into the difference equation the test component, we obtain

$$A\frac{\cos(k_x\Delta x)+i\sin(k_x\Delta x)-2G+G(\cos(k_x\Delta x)-i\sin(k_x\Delta x))}{\Delta x^2}\hat{\phi}_{i,j}^{n}+$$
$$\frac{G(\cos(k_y\Delta y)+\cancel{i\sin(k_y\Delta y)})-2G+G(\cos(k_y\Delta y)-\cancel{i\sin(k_y\Delta y)})}{\Delta y^2}\hat{\phi}_{i,j}^{n}=0$$

Solving for G

$$G=\frac{\cos(k_x\Delta x)+i\sin(k_x\Delta x)}{2-\cos(k_x\Delta x)+i\sin(k_x\Delta x)+\dfrac{2\Delta x^2}{A\Delta y^2}(1-\cos(k_y\Delta y))}$$

Note that the imaginary parts of the numerator and denominator are equal in magnitude. If we can show that the real part of the numerator is less than or equal in magnitude to the real part of the denominator, then the magnitude of G will be less than equal to one and hence, stability of the algorithm is proved. The magnitude of the numerator is bound by one and the real parts of the denominator are both positive and are bounded below by at least one

$$1\le 2-\cos(k_x\Delta x)+\frac{2\Delta x^2}{A\Delta y^2}(1-\cos(k_y\Delta y))$$

Thus $|G|\le 1$ and the subsonic difference equation of Murman-Cole is stable.

6.3.2 Supersonic Flow Case Stability

Again consider the equation in its linearized form, $A\phi_{xx}+\phi_{yy}=0,\quad with\quad A<0$, and differenced as follows

$$A\frac{\hat{\phi}_{i,j}^{n+1}-2\hat{\phi}_{i-1,j}^{n+1}+\hat{\phi}_{i-2,j}^{n+1}}{\Delta x^2}+\frac{\hat{\phi}_{i,j+1}^{n+1}-2\hat{\phi}_{i,j}^{n+1}+\hat{\phi}_{i,j-1}^{n+1}}{\Delta y^2}=0$$

All the superscripts in the above equation are $n+1$ and the relaxation index direction will not serve as the marching direction. But, this equation is actually marched in the x direction for the supersonic flow solution. Therefore, x is the time-like direction and we take $\phi_{i,j}=Gce^{ik_yy}$, $\phi_{i-1,j}=ce^{ik_yy}$ and $\phi_{i-2,j}=G^{-1}ce^{ik_yy}$. Upon substitution into the difference equation the test component, we obtain

$$A\frac{G-2+G^{-1}}{\Delta x^2}ce^{ik_yy}+\frac{G(\cos(k_y\Delta y)+\cancel{i\sin(k_y\Delta y)})-2G+G(\cos(k_y\Delta y)-\cancel{i\sin(k_y\Delta y)})}{\Delta y^2}ce^{ik_yy}=0$$

Solving for G

$$\underbrace{\left(1-\frac{\Delta x^2}{A\Delta y^2}(1-\cos(k_y\Delta y)\right)}_{a}G^2 \underbrace{-2}_{b}G+\underbrace{1}_{c}=0$$

The solution of the quadratic equation is $G=\dfrac{-b\pm\sqrt{b^2-4ac}}{2a}$, or

$$G=\frac{2\pm\sqrt{4-4\left(1-\dfrac{\Delta x^2}{A\Delta y^2}(1-\cos(k_y\Delta y)\right)}}{2\left(1-\dfrac{\Delta x^2}{A\Delta y^2}(1-\cos(k_y\Delta y)\right)}=\frac{1\pm\sqrt{\dfrac{\Delta x^2}{A\Delta y^2}(1-\cos(k_y\Delta y)}}{1-\dfrac{\Delta x^2}{A\Delta y^2}(1-\cos(k_y\Delta y)}=\frac{1\pm ig}{1+g^2},$$ where g is a real number. Therefore $|G|^2=\dfrac{1+g^2}{(1+g^2)^2}=\dfrac{1}{1+g^2}\le 1$ and the supersonic difference equation for the Murman-Cole algorithm is also stable.

6.4 Application of the Murman-Cole Method

Exercise: Solve the Transonic Small Disturbance equation for Case (1) subsonic flow with $M_\infty=0.735$ and Case (2) transonic flow with $M_\infty=0.908$, for flow past a 6% thick circular arc airfoil of chord length $c=1$, $th=0.06$, using the Murman-Cole method. Use a 51×51 mesh, with 21 equi-spaced points over the airfoil and stretched to far field boundaries 50 chord lengths away. Run each case 400 steps and plot c_p vs. x and the maximum residual vs. iteration step.

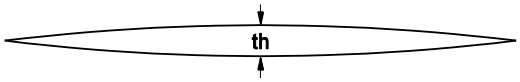

Figure 6.4 Symmetric circular arc airfoil.

Solution Approach: Assume we normalize pressure and density so that $V_\infty=1$, $\rho_\infty=1$ and $\gamma=1.4$. Then $a_\infty=V_\infty/M_\infty$ and $p_\infty=\dfrac{1}{\gamma}\rho_\infty a_\infty^2=\dfrac{1}{\gamma M_\infty^2}$. Because ϕ is the disturbance potential and not the full potential, we can use $\hat{\phi}=1$, or equal to any constant, as an initial condition.. Because of the symmetry of the flow, only the top or bottom half of the flow field needs to be calculated. We can place the chord line of the airfoil along the lower boundary given by $y=0$, place the top, left and right far field boundaries 50 chord lengths away and use the same mesh constructed in Section 5.3. Along the far field boundaries $\hat{\phi}$ is held constant and along the lower boundary the following condition on the derivative of $\hat{\phi}$ is used.

$$\frac{\partial\hat{\phi}}{\partial y}=V_\infty\left.\frac{dy(x)}{dx}\right|_{body} \quad for \quad 0\le x\le c \quad and \quad \frac{\partial\hat{\phi}}{\partial y}=0 \quad otherwise.$$

"Thin airfoil" theory is used to apply the boundary condition directly on the line $y = 0$, which includes the chord line, and not on the actual airfoil surface itself. Therefore, again there is no need for a body fitted mesh and a simple mesh aligned with the Cartesian coordinate system will suffice. The broken lines in the figure below indicate the extension to 50 chord lengths away from airfoil. The same mesh used previously for solving the model elliptic equation in Section 5.3 can be used here as well. Because the mesh is stretched, the Murman-Cole algorithm, defined herein for an equally spaced mesh, needs to use non-equally spaced difference approximations, as given in Section 3.3.

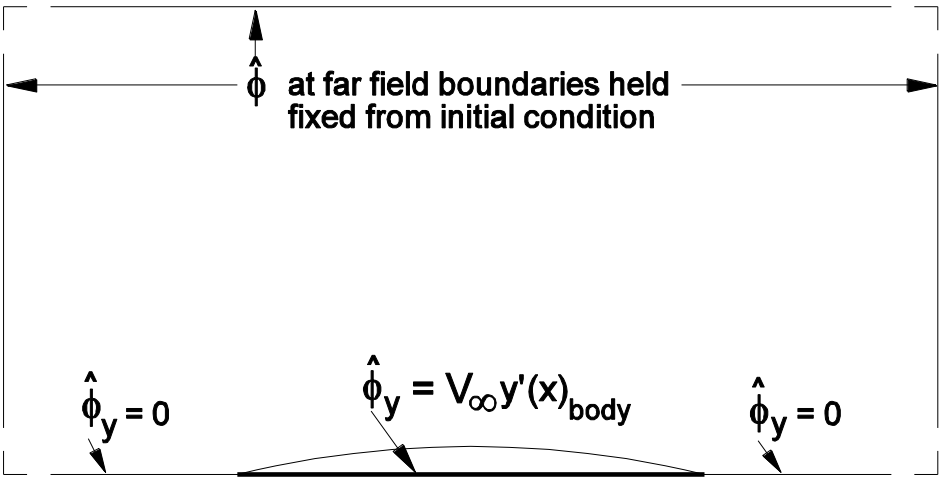

Figure 6.6 Flow volume about a symmetric circular arc airfoil

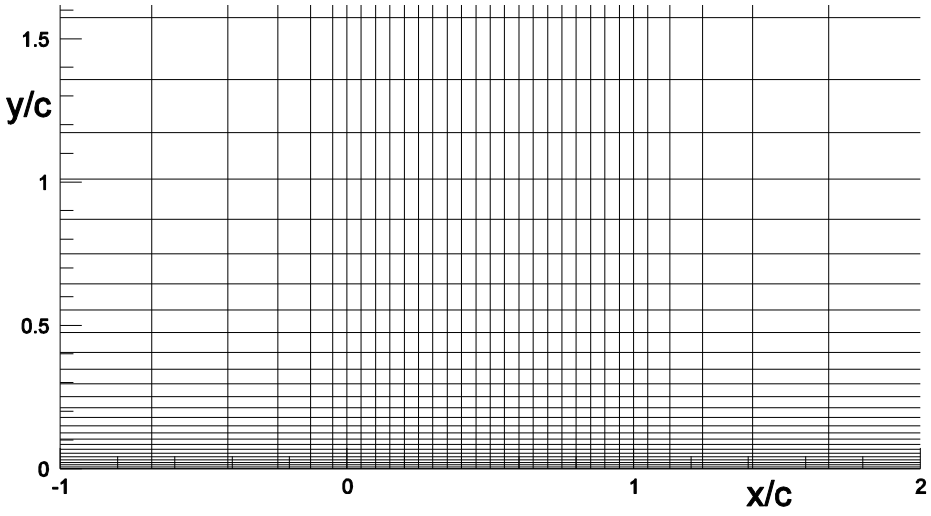

Figure 6.7 Mesh near airfoil

Exercise Results: The mesh near the airfoil surface is shown above and the pressure coefficient c_p, plotted with the negative c_p up, is shown below.

$$c_p = \frac{p - p_\infty}{\frac{1}{2}\rho_\infty V_\infty^2},\ p = p_\infty \left[1 - \frac{\gamma - 1}{2} M_\infty^2 \left(\frac{u^2 + v^2}{V_\infty^2} - 1 \right) \right]^{\frac{\gamma}{\gamma - 1}},\ u = V_\infty + \hat{\phi}_x \text{ and } v = \hat{\phi}_y .$$

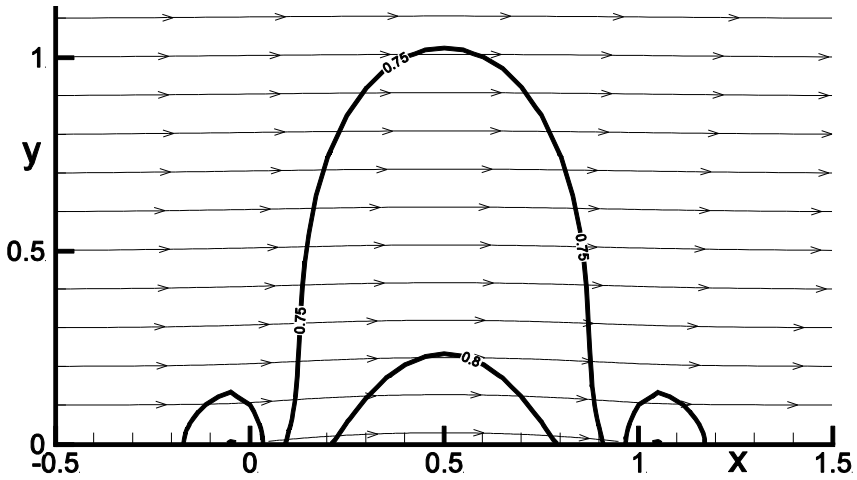

Figure 6.8 Case (1) Mach contours (0.7, 0.75 and 0.8) and streamlines for subsonic flow with $M_\infty = 0.735$

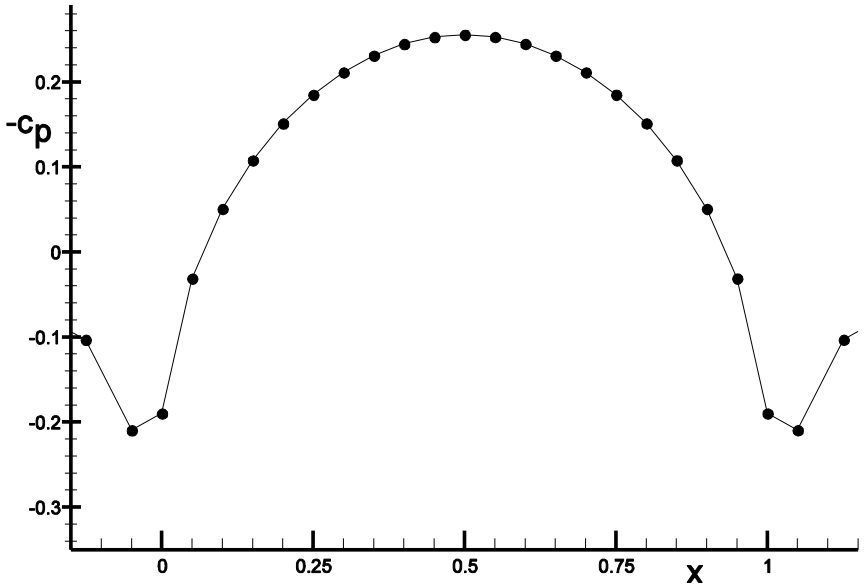

Figure 6.9 Case (1) c_p vs. x for subsonic flow with $M_\infty = 0.735$

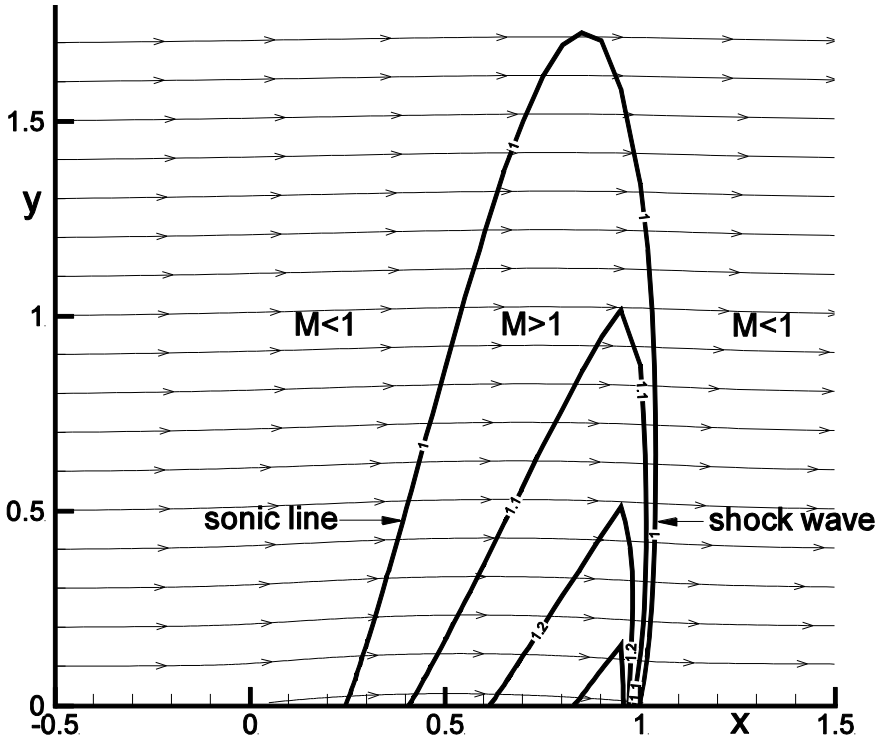

Figure 6.10 Case (2) Mach contours (1, 1.1, 1.2 and 1.3) and streamlines for transonic flow with $M_\infty = 0.908$

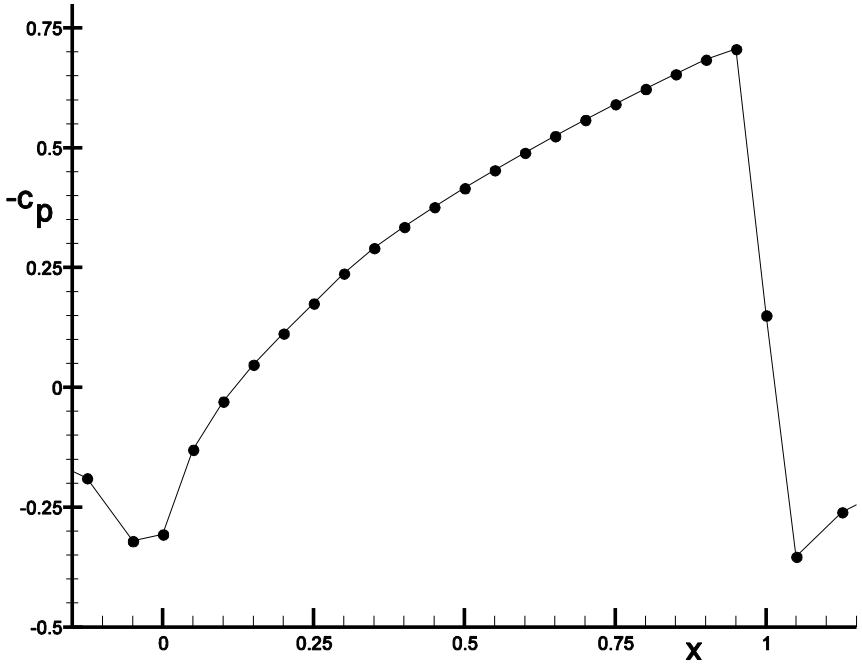

Figure 6.11 Case (2) c_p vs. x for transonic flow with $M_\infty = 0.908$

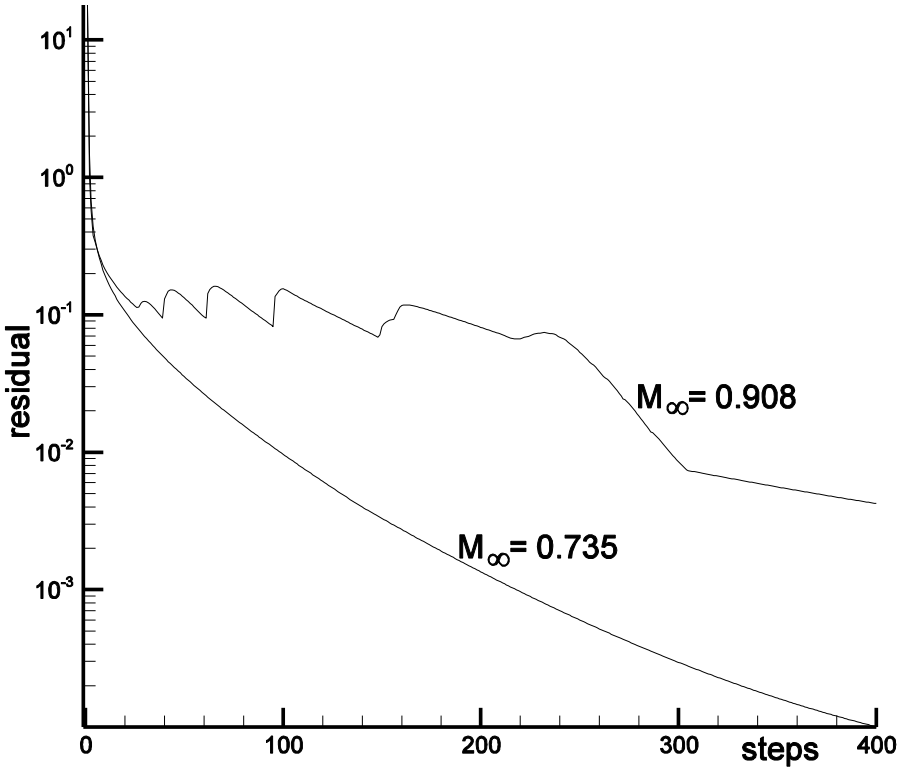

Figure 6.12 Maximum residual vs. x for $M_\infty = 0.735$ and $M_\infty = 0.908$

The maximum residual, $\max_{over\ i,j} \left| R_{i,j}^n \right|$, in the mesh versus iteration step is shown above for each case. Notice the smooth monotonic reduction in residual for the subsonic case and the non-monotonic wavy behavior for the transonic case. The behavior of the latter is caused by the shock wave at the trailing edge adjusting from one mesh point to another seeking its equilibrium position. (Don't worry if your transonic residuals look different from that shown. Small differences in programming can make large difference in residuals for flows containing moving shock waves.) Also note the perfectly symmetric c_p vs. x distribution for Case (1) containing only the subsonic flow and the very asymmetric Case (2) that generated supersonic flow about the airfoil.

The quality of the solutions obtained is not sufficiently accurate near the leading and trailing edges of the airfoil. The transonic case was repeated on an 101×51 mesh, with 61 mesh points spanning the chord line and stretched to refine the leading and trailing edge regions of the flow. The results are shown in Figures 6.13 and 6.14, after 5000 relaxation steps, close to convergence. Note the clear definition of the shock wave near the trailing edge.

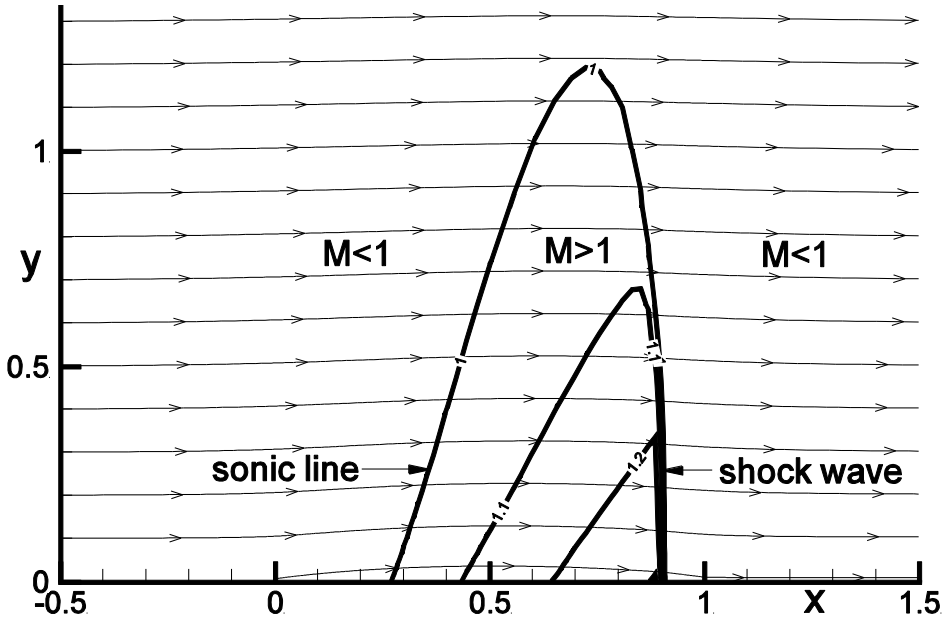

Figure 6.13 Case (2) Mach contours (1, 1.1 and 1.2) and streamlines for transonic flow with $M_\infty = 0.908$ on a 101×51 mesh

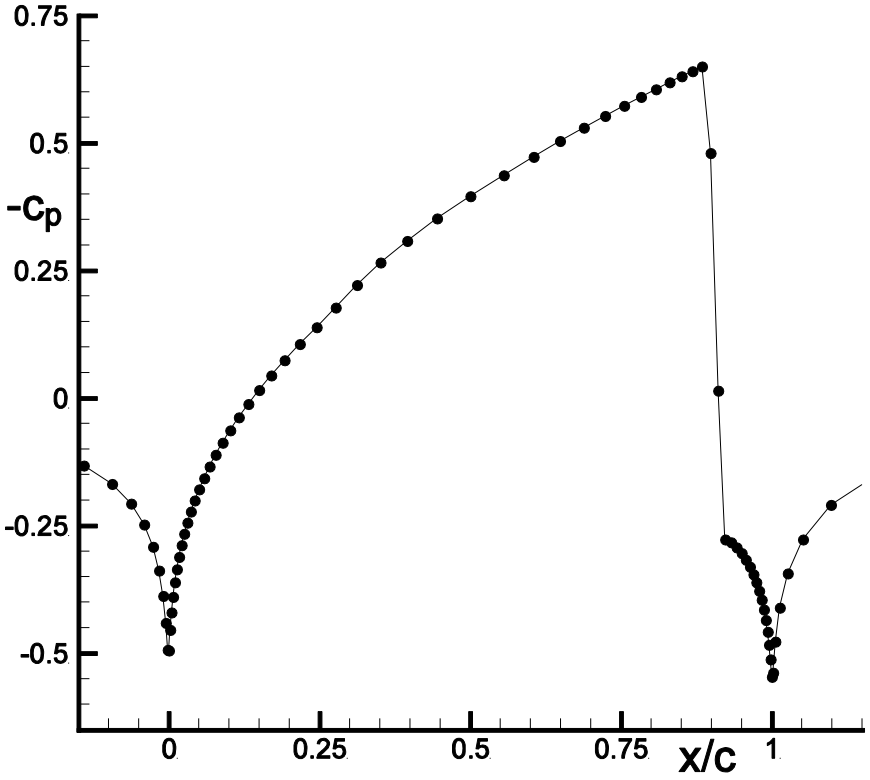

Figure 6.14 Case (2) c_p vs. x for $M_\infty = 0.908$ on a 101×51 mesh

The Murman-Cole procedure was a tremendous breakthrough for aerodynamicists. It also whetted their appetite for an algorithm for solving the next equation up on the hierarchical ladder – The Full Potential equation, which is not limited to small disturbances. Aerodynamicists next wanted to simulate the flow about blunt nose airfoils. The rush to apply the success of Murman and Cole proved to be more difficult than first thought and it took the genius of Antony Jameson to provide the next breakthrough. But, first we will need to consider coordinate transformations from physical space to computational space to avoid the limits of Cartesian meshes and to generate body fitted grids about blunt nosed airfoils. This will be done next in Chapter 7.

6.5 Correction Change or Delta Form of the Algorithm

The difference equation for the Murman-Cole algorithm is repeated below.

$$(1-\mu_{i,j}^{n})A_{i,j}^{n}\frac{\hat{\phi}_{i+1,j}^{n}-2\hat{\phi}_{i,j}^{n+1}+\hat{\phi}_{i-1,j}^{n+1}}{\Delta x^2}+\mu_{i-1,j}^{n}A_{i-1,j}^{n}\frac{\hat{\phi}_{i,j}^{n+1}-2\hat{\phi}_{i-1,j}^{n+1}+\hat{\phi}_{i-2,j}^{n+1}}{\Delta x^2}+\frac{\hat{\phi}_{i,j+1}^{n+1}-2\hat{\phi}_{i,j}^{n+1}+\hat{\phi}_{i,j-1}^{n+1}}{\Delta y^2}=0$$

Again the terms known from previous line solutions are then moved to the right hand side of the equation to obtain.

$$(1-\mu_{i,j}^{n})A_{i,j}^{n}\frac{-2\hat{\phi}_{i,j}^{n+1}}{\Delta x^2}+\mu_{i-1,j}^{n}A_{i-1,j}^{n}\frac{\hat{\phi}_{i,j}^{n+1}}{\Delta x^2}+\frac{\hat{\phi}_{i,j+1}^{n+1}-2\hat{\phi}_{i,j}^{n+1}+\hat{\phi}_{i,j-1}^{n+1}}{\Delta y^2}=$$

$$-(1-\mu_{i,j}^{n})A_{i,j}^{n}\frac{\hat{\phi}_{i+1,j}^{n}+\hat{\phi}_{i-1,j}^{n+1}}{\Delta x^2}-\mu_{i-1,j}^{n}A_{i-1,j}^{n}\frac{-2\hat{\phi}_{i-1,j}^{n+1}+\hat{\phi}_{i-2,j}^{n+1}}{\Delta x^2}$$

A tridiagonal matrix was then formed for relaxing the solution, a line of which is shown below, until the residual $R_{i,j}^{n}$ converged to zero.

$$b_{i,j}\hat{\phi}_{i,j+1}^{n+1}+a_{i,j}\hat{\phi}_{i,j}^{n+1}+c_{i,j}\hat{\phi}_{i,j-1}^{n+1}=f_{i,j}$$

$$R_{i,j}^{n}=(1-\mu_{i,j}^{n})A_{i,j}^{n}\frac{D_{xx}\cdot}{\Delta x^2}\hat{\phi}_{i,j}^{n}+\mu_{i-1,j}^{n}A_{i-1,j}^{n}\frac{D_{xx}\cdot}{\Delta x^2}\hat{\phi}_{i-1,j}^{n}+\frac{D_{yy}\cdot}{\Delta y^2}\hat{\phi}_{i,j}^{n}$$

It is more convenient and safer to construct algorithms that compute the change to the present solution, $\delta\hat{\phi}_{i,j}$, at each step rather than the new solution, $\hat{\phi}_{i,j}^{n+1}$ itself. This type of algorithm takes on the following form for the Transonic Small Disturbance equation solved by the Murman-Cole Method.

$$b_{i,j}\delta\hat{\phi}_{i,j+1}^{n+1}+a_{i,j}\delta\hat{\phi}_{i,j}^{n+1}+c_{i,j}\delta\hat{\phi}_{i,j-1}^{n+1}=R_{i,j}^{n}\ \text{ with }\ \hat{\phi}_{i,j}^{n+1}=\hat{\phi}_{i,j}^{n}+\delta\hat{\phi}_{i,j}^{n+1}$$

The scalar tridiagonal matrix elements $a_{i,j}$, $b_{i,j}$ and $c_{i,j}$ are the same as before. The pro's use this form because if the algorithm converges, $\delta\hat{\phi}_{i,j}\to 0$ for all i, j, then the residual

is also driven to zero, i.e. $R_{i,j}^{n}$ vanishes. Therefore the converged solution satisfies difference equation, together with all boundary conditions, even when errors have been accidentally introduced into the matrix elements above or when these elements are purposely modified to improve the rate of convergence.